From DEPARTMENT OF CLINICAL SCIENCE, INTERVENTION AND TECHNOLOGY, DIVISION OF RADIOGRAPHY
Karolinska Institutet, Stockholm, Sweden

THE DEPENDENCY OF IMAGE QUALITY ON ACQUISITION PROTOCOL AND IMAGE PROCESSING IN CHEST TOMOSYNTHESIS

Masoud Jadidi

Stockholm 2019

Cover illustration:

The lung images are provided by my supervisor, Sven Nyrén, from the PACS system at Karolinska University Hospital in Solna. The images are selected from one individual included in the study. The protocol conditions and image processing parameters are representing the creation of different type of chest digital images. The background image is a public image which is downloaded from the social network, Flickr through the Karolinska Institutet website.

Published by Karolinska Institutet

ISBN 978-91-7831-354-9
Printed by E-Print AB 2019

To my life-partner, best friend, source of inspiration and soulmate who believes in me no matter who I am, and encourages me to follow my dreams.

THE DEPENDENCY OF IMAGE QUALITY ON ACQUISITION PROTOCOL AND IMAGE PROCESSING IN CHEST TOMOSYNTHESIS

THESIS FOR LICENTIATE DEGREE

By

Masoud Jadidi

Huvudhandledare:
Doc. Sven Nyrén
Karolinska Institutet
Department of Molecular Medicine and Surgery

Karolinska University Hospital
Department of Thoracic Radiology

Bihandledare:
Prof. Magnus Båth
Sahlgrenska Academy at University of Gothenburg
Department of Radiation Physics

Sahlgrenska University Hospital
Department of Medical Physics and
Biomedical Engineering

Prof. Anders Sundin
Uppsala University Hospital
Department of Radiology Department

Uppsala University
Department of Radiology, Oncology and
Radiation Science

Kent Fridell, PhD
Karolinska Institutet
Department of Clinical Science, Intervention and
Technology (CLINTEC)

Betygsnämnd:
Prof. Örjan Smedby (samordnare)
KTH
Department of Biomedical Engineering and
Health systems
Division of Centre for Life Sciences Imaging at
KTH Karolinska

Doc. Marcus Söderberg
Lunds University
Department of Translational Medicine
Division of Medical Radiation Physics

Doc. Samy Abdel Halim
Karolinska University Hospital,
Department of Lung Oncology Center
Division of Cancer

ABSTRACT

The digital tomosynthesis (DTS) technique is a next generation of the old tomography technique, the use of which has been extended during the past decade. The interest in this technique has increased more and more in Radiology due to its ability to provide three-dimensional images by acquiring a number of projection radiographs at lower radiation dose and potentially lower cost than CT in certain clinical situations. Furthermore, there are two main advantages of DTS in comparison with conventional radiography. The first one is that the reconstructed slices reduce the problem of overlaying anatomical structures in a two-dimensional image created by conventional radiography. The second one is that DTS has better depth resolution than conventional radiography.

The primary aims of the studies in this thesis have been to determine a chest DTS protocol with shorter exposure time then the vendor recommended protocol (12 s) with retained image quality and to investigate the difference in image quality between the protocols with acquisition time 6.3 s and 12 s.

In order to compare all available chest DTS protocols, an anthropomorphic phantom with a 12 mm module placed in the center of the right lung was used for the first study. The second study was performed as a prospective human study where the best performing protocols from the first study were compared. In both studies, the observers were instructed to evaluate the image quality based on the pre-defined criteria. The criteria were developed in accordance with the European guidelines and previous studies in combination with the clinical experience of the observers. The data from both studies were analysed with visual grading characteristics (VGC) analysis and the area under the VGC curve (AUG_{VGC}) was used as figure-of-merit.

The result of the studies indicates that the chest DTS protocol with the acquisition time of 6.3 s has similar image quality as the reference protocol with acquisition time of 12 s for all quality criteria. The shorter acquisition time may have a great clinical significant for the patient with respiratory impairment.

In the future, further studies should be performed to evaluate the diagnostic value of chest DTS in compare with CT in some clinical situations, reduction of radiation dose and cost efficiency within healthcare.

ACKNOWLEDGMENT

It is my great pleasure to express my deep sense of gratitude and respect to my principal supervisor, Dr. Sven Nyrén, for infusing confidence and inspiring me in my work, through his encouragement and guidance. It would never have been possible for me to take this thesis to completion without his incredible support and encouragement.

My respectable gratitude and heart full thanks to my co-supervisor, Prof. Magnus Båth for helping me to stay on track in my studies and valuable suggestions and feedbacks on manuscripts and this thesis. It has been an honour and a real privilege for me to get a share of his exceptional scientific knowledge.

I also would like to thank to my co-supervisor Prof. Anders Sundin for his constant support and availability for evaluation of digital tomosynthesis images but also for his constructive suggestions for the accomplishment of the work presented in this thesis.

A special thanks to my co-supervisor, Dr. Kent Fridell, the first person who encouraged and supported me in my academic journey and always ready to help me.

I am thankful to Dr Jacek Pawlowski and Prof. Peter Aspelin for evaluation of digital tomosynthesis images.

I take this opportunity to extent my gratitude to Farzaneh Farizandi, MSc, for performance of tomosynthesis examinations, Maria Marteinsdottir, MSc, for calculations of effective dose and additional, Mrs. Kerstin Edwall and Mr. Mikael Lindberg for organizing the image collection in the PACS system.

LIST OF SCIENTIFIC PAPERS

I. Jadidi M, Sundin A, Aspelin P, Båth M, Nyrén S**.** Evaluation of a new system for chest tomosynthesis: aspects of image quality of different protocols determined using an anthropomorphic phantom. Br J Radiol. 2015;88(1053):20150057.

II. Jadidi M, Båth M, Nyrén S. Dependency of image quality on acquisition protocol and image processing in chest tomosynthesis-a visual grading study based on clinical data. Br J Radiol. 2018; 91(1087):20170683.

CONTENTS

LIST OF ABBREVIATIONS

AUC	Area Under the Curve
CR	Computed Radiography
CsI	Caesium Iodide
CT	Computed Tomography
DTS	Digital Tomosynthesis
CXR	Chest Radiography
FBP	Filtered Back Projection
FNC	Flexible Noise Control
FPD	Flat Panel detector
GP	Gradation Processing
ID	Identity
ISS	Irradiation Side Sampling
MFP	Multi-Objective Frequency Processing
MRI	Magnetic Resonance Imaging
PA	Poster Anterior
PACS	Picture Archiving and Communication System
PET	Positron Emission Tomography
SAA	Shift-and-Add
SID	Source to Image Distance
SDD	Source to Detector Distance
VGC	Visual Grading Characteristics

1 INTRODUCTION

The two main X-ray based modalities, conventional radiography and computed tomography (CT), have traditionally been the most commonly used radiological examinations in thorax radiology in hospitals around the world. For the majority of pulmonary diseases, chest radiography still remains the preferred first go-to radiological examination. At the department of radiology, Karolinska University Hospital, Stockholm, Sweden, 42,848 chest radiography examinations and 24,804 Chest CT examinations were performed in 2018. The main advantage of chest radiography is high accessibility, cost-effectiveness, low radiation dose and short examination time. The detectability of pathologic findings due to overlaying of anatomic structures is however a known limitation of chest radiography[1-4]. Since the introduction of CT in the 1970s, some of CT's clinical advantages have exceeded some of the disadvantages of chest radiography. On the other hand, the rapid increase in use of CT has exposed both adults and children to increased amounts of radiation and thus an increased risk of developing cancer. Although Low-dose CT has been evaluated clinically for detection of lung nodules in lung cancer screening, it is still an expensive examination with lower accessibility than conventional radiography[5,6].

The digital tomosynthesis (DTS) technology is used for high-resolution and limited angle tomography and was developed based on the old technique of geometric tomography. DTS does however use a higher radiation dose, compared to conventional chest X-ray, hence additional studies are needed to determine an acceptable dose level for clinical use. DTS has been clinically evaluated and approved for a variety of clinical applications such as orthopedic imaging, dental imaging, angiography, mammographic imaging, pediatric esophageal foreign body and chest imaging[6-8]. The interest in using DTS in detecting lung nodule has increased significantly[6,9]. Given the challenges of conventional chest radiography in detecting pulmonary nodules, previous studies have shown significantly higher sensitivity in detection of pulmonary nodules with DTS, compared to chest radiography[3,10-12]. While DTS has inferior nodule detection sensitivity compared to CT, DTS may be beneficial as a low-dose alternative to chest CT for follow up of existing pulmonary nodules[13,14].

Chest DTS is performed by using conventional chest radiography equipment, although some modification is needed to allow the X-ray tube to move in one direction during the exposure to acquire projection images within a limited angular range. These projection images are used to reconstruct tomographic planes at different depths, providing a three- dimensional image of the chest. This provides a solution to overlapping anatomy with the effective dose to a standard-sized patient (170 cm/70 kg) being only slightly higher compared to conventional two-view chest radiography examinations[15-19].

Several technological improvements within the last two decades have made tomosynthesis clinically beneficial. Some significant advances have been the development of Flat-Panel Detectors (FPD) with high detective quantum efficiency; development of reconstruction accuracy and development of acquisition parameters[6,20].

1.1 HISTORICAL BACKGROUND OF TOMOSYNTHESIS

In 1921, the French man André Edmond Marie Bocage applied for a patent on a technique called planigraphy. The technique was based on a simultaneous movement of the X-ray tube and X-ray film in a synchronized motion during exposure. This technique makes the structures within a specified plane parallel to the movement direction of the X-ray source and X-ray film in focus while the other planes in the volume remain blurred. During the same year, the Dutch researcher Bernard Ziedses des Plantes claimed that he invented the method independently. But the basic theoretical framework for limited angle tomography was published in 1931 and Ziedses des Plantes was the first person to actually perform experimental work[21]. This was the first step to obtain three-dimensional images of the interior of the human body, and tomography was endorsed as a new radiological examination (Figure 1.1). However, there were specific limitations on the use of tomography. First of all, in order to visualize an additional plane in the volume, a new exposure was required. Secondly, compared to conventional X-ray images, with this technique it was not possible to completely suppress residual blur from out-of-plane structures[6,21-23].

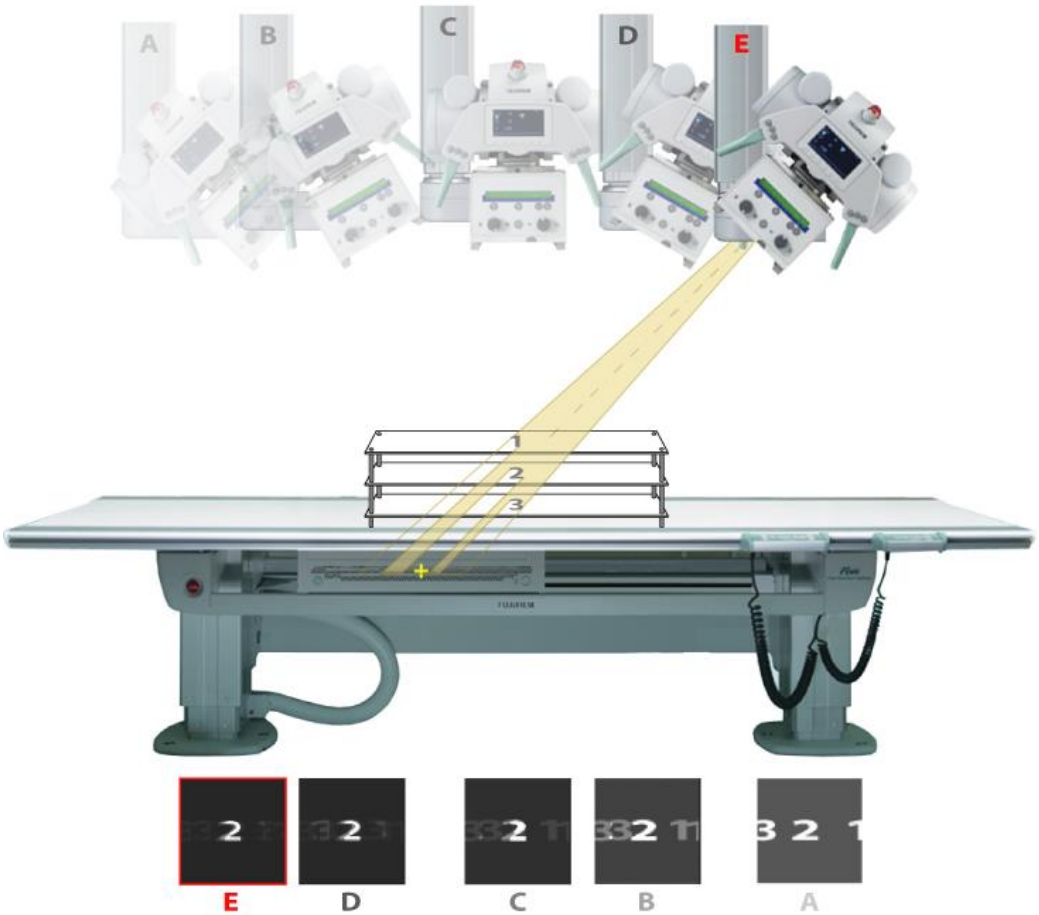

Figure 1.1 Illustration of the tomography technique. The X-ray film accumulates image data through the exposure. E.g. image A is a single exposure image where one continuous exposure is made as the X-ray tube moves from one end of the table to the other. Figure was derived with permission from Fujifilm, Stockholm, Sweden.

In 1934, Bernard Ziedses des Plantes described the technique of shift-and-add (SAA) in order to solve the first drawback of tomography[21]. He meant that by summing up all the separate acquired projection images at different depths in a volume, one specific plane in the subject will be in focus while all the other plane will remain blurred. Projection images from different depths in the body can be obtained by shifting the individually acquired images relative to each other before each summation (Figure 1.2)[6,22,23].

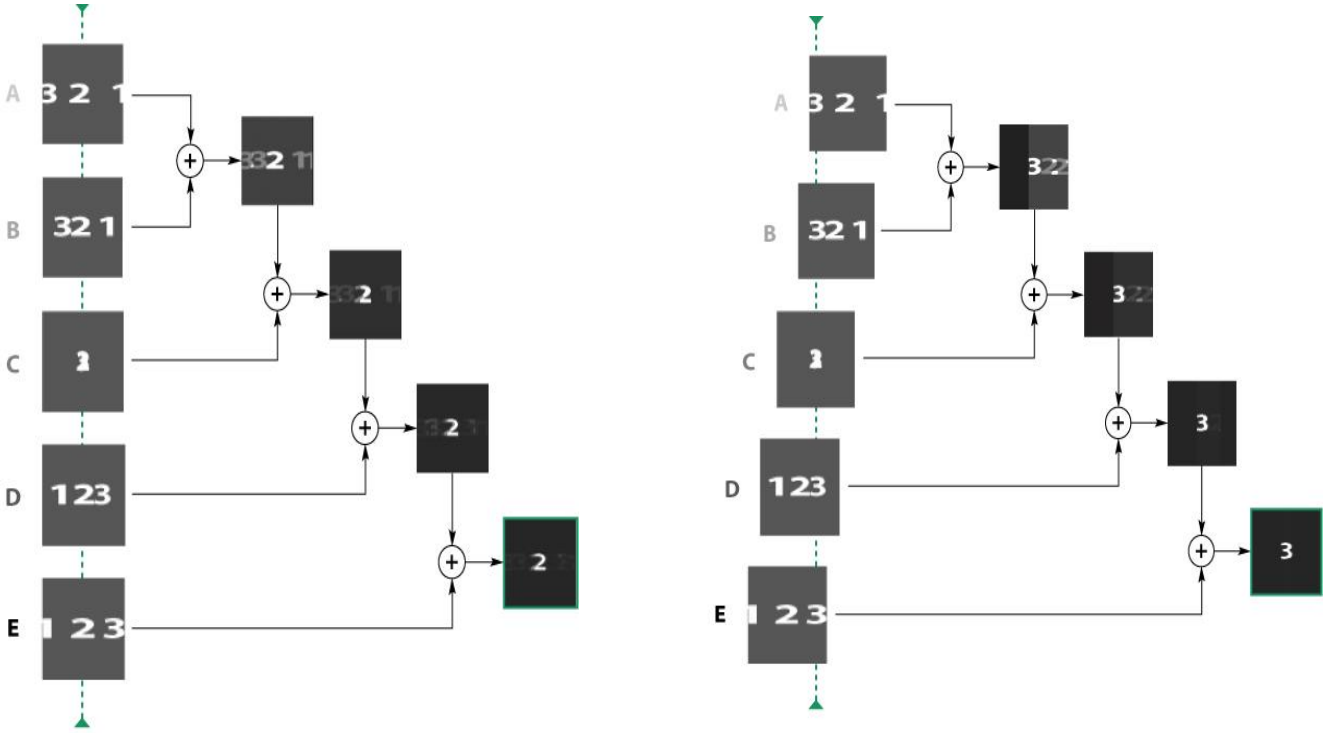

Figure 1.2. Illustration of the shift-and-add technique. By shifting the individually acquired images relative to each other before summation, objects from different planes in the body part are apparent while the objects in other planes will be blurred. Figure was derived with permission from Fujifilm, Stockholm, Sweden.

In 1969, based on the Ziedses des Plantes' theory, Garrison et al. built a prototype system called "three-dimensional roentgenography". After his try with the prototype, he mentioned that the residual blur from out-of-plane structures can be reduced by image processing[21,24,25]. In the early 1970s, Grant introduced the term "tomosynthesis", from the Greek words "tomo" and "synthesis". "Tomo" means cut, slice or section and "synthesis" from the ancient Greek and means "combination" or "composition". In 1972, he evaluated the first digital tomosynthesis system[21,26].

In the 1970s and 1980s, the focus was mainly on sophisticated approaches to improve image quality by deblurring algorithms. In the development of the tomosynthesis technique, an additional challenge was the lack of appropriate digital detector technology for acquisition of the projection images[6,21,27].

There is an essential difference between tomography and tomosynthesis techniques. In tomography, one continues exposure is made as the X-ray tube moves from one end of the detector to the other, and the detector accumulates image data throughout the exposure (Figure 1.1). However, with the tomosynthesis technique, individual and short duration exposures are made as the X-ray tube moves from one end of the detector to the other, and the detector acquires an individual image from each exposure (Figure 1.3).

In the 1990s a new generation of flat-panel detectors (FPDs) was introduced. This, in combination with modern computer technology, solved the problems of poor image quality and long examination times which was a disadvantage with the older tomography techniques.

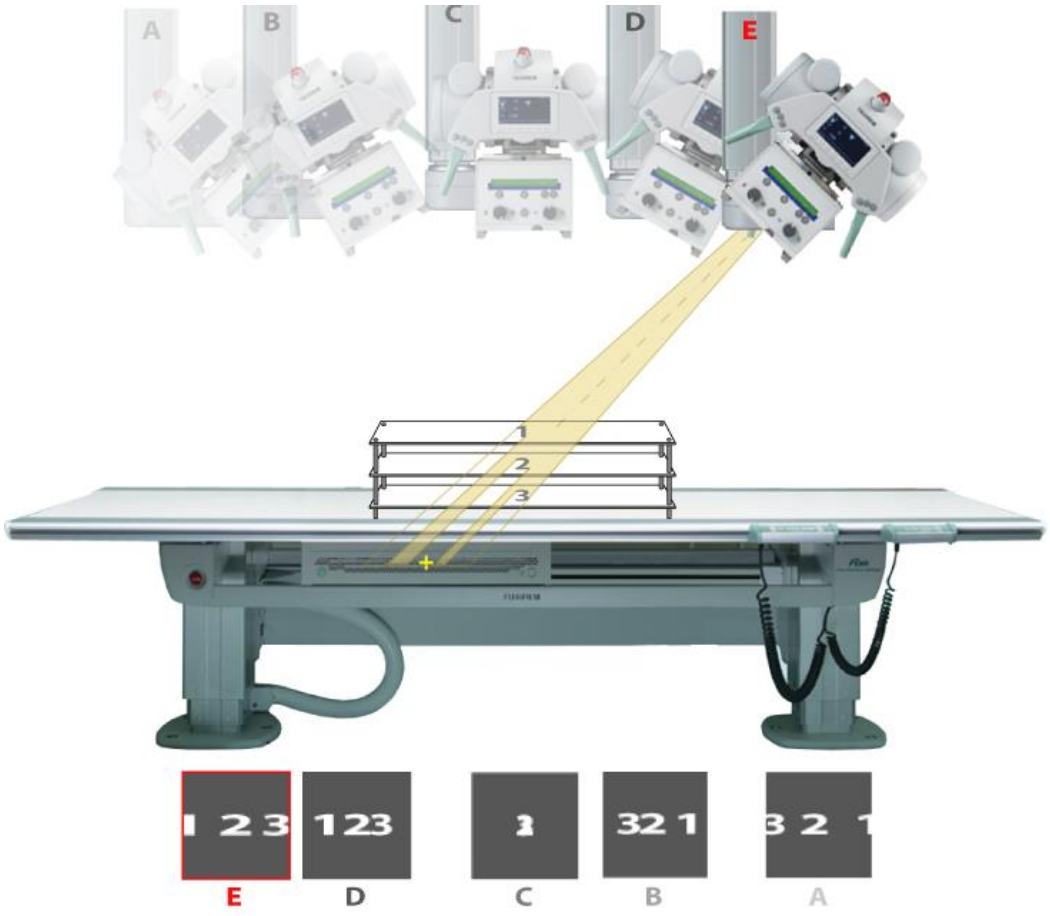

Figure 1.3 Illustration of the DTS technique. The detector acquires an individual image for each exposure at different angles as the x-ray tube moves from one end of the table to the other. Later on, the individually acquired images are combined to produce the tomosynthesis images. Figure was derived with permission from Fujifilm, Stockholm, Sweden.

1.2 CHEST TOMOSYNTHESIS TODAY

Fujifilm Corporation, Medical System Business Division introduced the DTS system (FDR AcSelerate) at the Radiological Society of North America (RSNA) 2011. Fujifilm is the third medical company to develop a DTS system for thoracic radiology (e.g. lung nodule, pleura

lesion) and orthopaedics (e.g. rheumatic bone erosion, narrowed knee joint cavity and spine shape diagnosis). DTS has been shown to be of special value in the diagnosis of some bone fractures (e.g. scaphoid), in otology (paranasal sinuses) and contrast radiography (cholecystography, digestive tract). The tomosynthesis option could be implemented on the chest and table unit in order to perform DTS examinations in the standing-up position (e.g. for chest DTS) or lying position (for e.g. spine DTS). Depending on the patient position, the X-ray tube moved either vertically or horizontally and acquired an individual image for each exposure (between 20-60 exposures) in the angulation interval 10°-27° over 4-12 seconds, depending on the tomosynthesis protocol.

Other commercially available DTS systems are

- the GE Definium 8000 system with VolumeRAD option (GE Healthcare, Chalfont St. Giles, UK), aimed as conventional digital radiographic imaging with option of DTS technology.
- the SonialVision Safire system (Shimadzu Co., Kyoto, Japan), designed as a digital fluroscopy system with the additional option of DTS functionality. Compared with other systems, for performance of the stand tomosynthesis examination, the fluroscopy table should be tilted.

The system function of GE's chest unit is the same as Fujifilm's system, which is a linear movement of the X-ray tube applied at different angles with a stationary detector. However, in the Shimadzu system, the detector and the X-ray tube have a linear movement in opposite directions[10,11,20,28].

The common workflow for all suppliers is that the projection images are subsequently reconstructed into a 3D volume on the reconstruction unit and the standard Filtered Back Projection (FBP) algorithm is used in order to decrease blurred out-of- plane subjects.

1.2.1 Technology of Flat Panel Detector (FPD)

Image quality is an important attribute of chest tomosynthesis imaging and the development of the flat panel detector´s characteristics has played an important role in achieving the optimum image quality for diagnostic use. This implies that the development of the FPD is likely to continue in the coming years.

Today's most common DTS systems, with an up-right position for chest tomosynthesis and a table top position for bedside tomosynthesis examinations, are designed based on a fixed FPD with a parallel-path motion X-ray tube (Figure 1.3). The parallel-path motion with fix FPD prevents non-stationary detector response, enables faster acquisition time due to a continuous X-ray tube motion and creates the easiest reconstruction algorithm, thus leading to similar magnification at each tube position[22,29].

Currently, there are two major detector technologies, called direct and indirect conversion. The indirect conversion technology converts X-ray to light by a scintillator and the light is then transformed to an electric signal for digitalization using a photodiode. The direct conversion technology uses a semi-conductor material for signal acquisition and digitization directly from x-ray[28,30]. The most common detector material for DTS system is Caesium Iodide (CsI), known as indirect detector which is used by GE and Fujifilm. However, Shimadzue uses Amorphous Selenium (a-Se), known as direct detector in its DTS system.

The latest detector technology development has been focused on the CsI detector. The conventional Caesium Iodide (CsI) FPD converts the X-ray photons to visible light photons in a scintillator and then the light photons are converted into electrical charge and read out by Thin-Film-Transistor (TFT) array bonded to the scintillator. The fundamentals of this technology is that light photons transmit through the CsI layer and when they reach the CsI phosphor base, poor- crystallized section, these light photons may spread laterally and decrease in intensity. The disadvantage is that the base of the columnar is flared and suffers from poor crystallinity and when the crystals are fused together, it may cause signal loss and more blur (Figure 1.4).

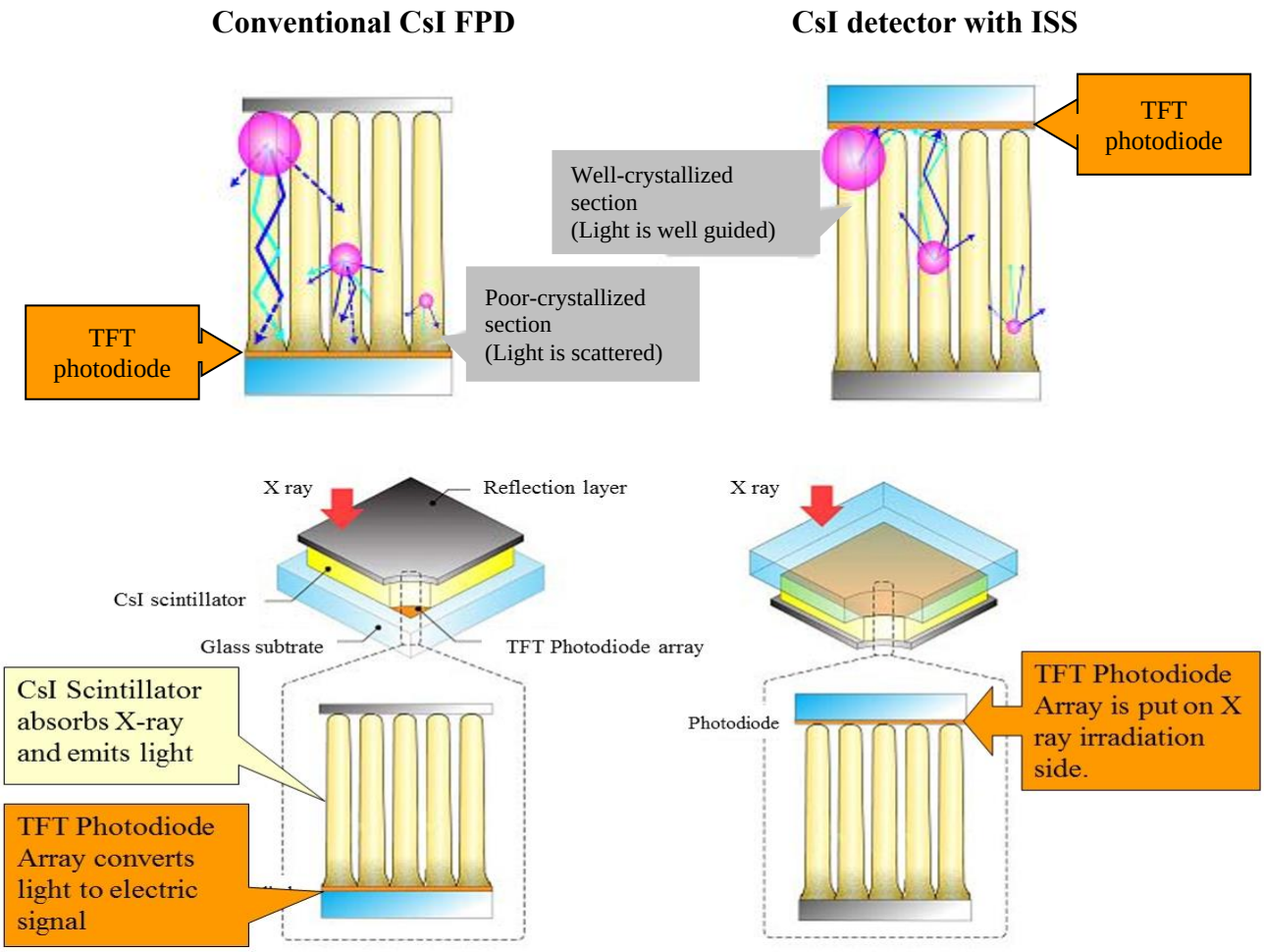

Figure 1.4. Conventional CsI FPD and CsI FPD with ISS technology. Information was derived with permission from Fujifilm, Stockholm, Sweden.

To overcome this drawback, Fujifilm developed a new type of CsI FPD with its proprietary sampling technology, “Irradiation Side Sampling” (ISS), to achieve the appropriate image quality. The CsI TI detector is dipped in Tallium salt and the TFT photodiode is adhesively coupled to the X-ray irradiation side – which has a well-crystalized section. This means that the readout occurs on the exposure entrance side of the detector, where the light is well guided. (Figure 1.5).

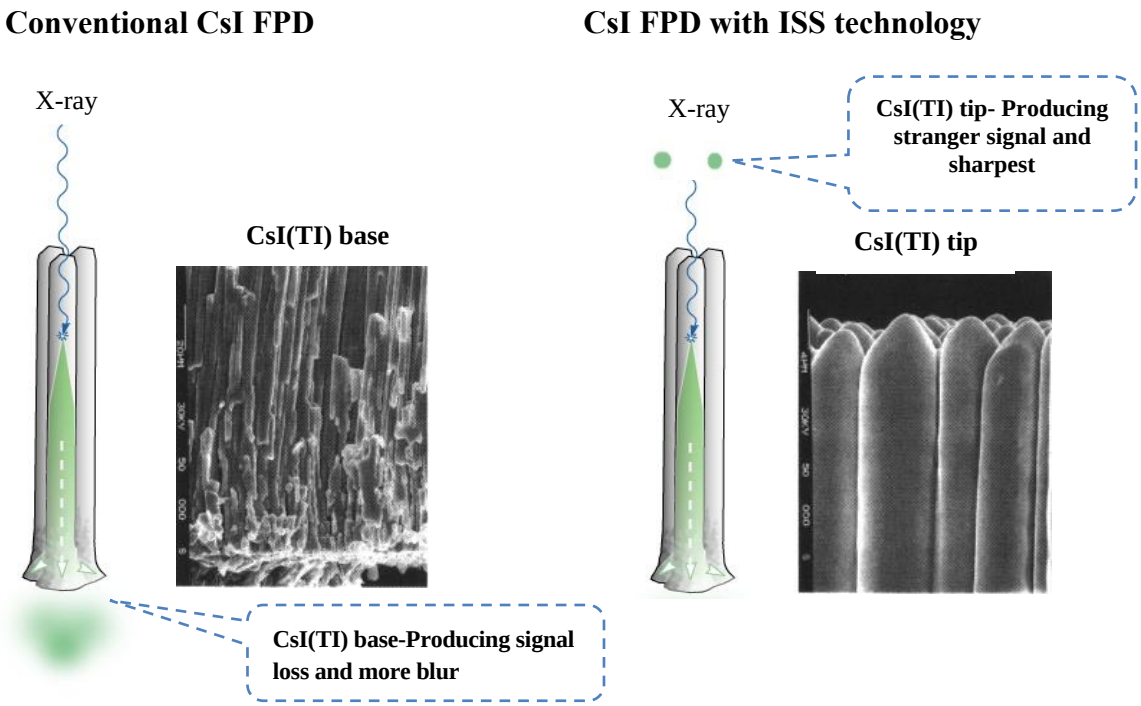

Figure 1.5. The structure of CsI TI FPD. Information was derived with permission from Fujifilm, Stockholm, Sweden.

1.2.2 Image processing parameters

In 1983, Fujifilm Medical Co., Ltd. (Tokyo, Japan) introduced the first Computed Radiography (CR) as a diagnostic radiographic system with only two image processing technologies: Gradation Processing (GP) and Spatial Frequency Processing. By that time the image processing parameters for conventional chest radiography were already used to enhance the structures in the lungs, mediastinum, heart, skeleton and upper abdomen. In 1999, a new image processing technology called Multi-Objective Frequency Processing (MFP) was developed. Finally in 2005, an additional image processing technology, Flexible Noise Control (FNC) was introduced by Fujifilm[31-33].

GP is controlled by four different parameters which convert the digital input data (raw data) to a conventional image with appropriate contrast and density. The aim of using 6 parameters of MFP is to enhance the visibility of both dense and peripheral tissue by using various degrees of contrast and frequency on different-sized structures in the same image. The four parameters

of FNC enables noise data to be extracted and suppress the noise level in all density areas, especially those with medium to low dose, without losing the sharpness[16,31,32]. All parameters are listed, together with a short description in Appendix 1[16].

1.2.3 Chest tomosynthesis protocols

The Fujifilm DTS system is supplied with a large number of tomosynthesis protocols (called tomosynthesis exposure identity (ID) by the vendor) for different anatomy such as pelvis, spine, hip joint and chest.

The variety of the protocols allows the operator to select the appropriate protocol dependent on the patient's condition and clinical requirements. For the chest tomosynthesis, the system offers different options of DTS protocols, incl. vendor recommended exposure ID 76. The exposure conditions for each exposure ID consist of source-to-image distance (SID) of 130 or 180 cm, X-ray tube swing angle, total exposure time, tube voltage, tube current and the filtration (Appendix 2). For both studies, the tube voltage (kV) and a total filtration of 3.5mm Al plus 0.2mm Cu were kept constant, but the tube current (mA) was adjusted for each protocol in order to achieve a constant effective dose of 0.4mSv for each protocol. Furthermore, other settings such as collimation of the X-ray tube, reconstruction settings and image post-processing parameters were kept the same for all protocols. The X-ray tube moves vertically and acquired 20–60 exposures in the angular interval 10°–27° over 4–12 s, depending on the selected protocol. Two different grids, with aluminum interspace, were used: a grid with ratio 10/1 and a focusing distance of 140cm for protocols with SID 130cm and a grid with ratio 12/1 and a focusing distance of 180cm for protocols with SID 180cm[15,16].

1.3 CLINICAL EVALUATION OF CHEST TOMOSYNTHESIS

Given that lung cancer has had the highest mortality rate of all cancer types for many years[34,35], the accuracy in detectability of pulmonary diseases, in order to improve diagnostic performance, is very important. Based on commercially available tomosynthesis system, some clinically related research studies have been conducted comparing the sensitivity of conventional chest radiography and chest tomosynthesis as they relate to pulmonary diseases, such as mycobacterial inflammation, fibrosis or a combination[36,37]. Other challenges for the diagnosis of pulmonary diseases include accurately characterizing the lung nodules, due to the large variety of histological entities. Clinically the key task is the classification into benign or malignant lesions. The high sensitivity and specificity in detecting malignance, especially in the solitary pulmonary nodule is therefore the main aim of using different imaging modalities for this purpose[34,35,38,39].

Different imaging modalities perform differently in terms of pulmonary nodule detection. Conventional Chest radiography has relatively low detectability for the solitary pulmonary nodule, e.g. detection of solitary nodules of size <5 mm is rare and detectability of nodule with size of 6-10 mm is 50%. However, magnetic resonance imaging (MRI) has sensitivity of >

50% for nodules size >5 mm and almost 100% for nodules size of >10 mm. CT has been the gold standard for detection of pulmonary nodules with a sensitivity of 95% for nodules >5 mm and 100% for nodules >10 mm. Furthermore, the technology of spiral multi-detector CT is even able to disclose nodules sized 1-2 mm. Positron emission tomography (PET) has showed a sensitivity of 95%, specificity of 87% and accuracy of 92% for detection of solitary nodules[39]. In an observer study of clinical cases by Vikgren et al, the authors reported on the performance of chest DTS for detection of pulmonary nodules compared to chest radiography with CT as reference. For DTS, the visibility of the nodules ≤ 4 mm was 86%, for nodules >4-6 mm, 91% and for nodule >6 mm visibility was 100%[3]. Another study by Meltzer et al presented the detection and characterization of solid pulmonary nodules at DTS, on the CT-proven nodules. The result showed that the detection rate of the nodules ≥ 5 mm and ≥ 6 mm, was, 49%-58% and 48%-62%, respectively. Based on the detection rate of solid pulmonary nodules, Meltzer suggested to use DTS for follow-up to CT[14]. Apart from these comparative studies, some studies have been conducted to determine the benefits of DTS technique and to investigate the clinical added value in the diagnosis of pulmonary lesions and pulmonary disease.

The common conclusion of those studies is that DTS is a sensitive imaging technique which improves diagnostic accuracy of pulmonary lesions. Furthermore, DTS was clinically comparable to chest CT for lung metastases in patient with colorectal cancer[40-43].

In the work presented in this thesis, different chest protocols of a new DTS system were evaluated in order to determine a chest protocol with the highest clinical benefit in terms of shorter acquisition time with maintained image quality. The studies are neither a comparison of DTS with other radiology techniques (radiography, CT, MRI and PET), nor a comparison of those techniques in detecting of pulmonary nodules. Due to the development of a series of acquisition protocols in a new DTS system, the evaluation of the overall chest image quality was the main purpose of these studies.

1.4 IMAGE QUALITY CRITERIA FOR CHEST TOMOSYNTHESIS

The image quality evaluation is based on two general guidelines outlining the quality criteria for diagnostic radiography and CT. These guidelines came to fruition through Europe-wide cooperation between diverse professionals and authorities in the field of diagnostic radiology and diagnostic CT[44,45]. There are also criteria for tumor response. In 1981, the first criteria for tumor response were introduced by the World Health Organization (WHO) where tumor response was measured in patients with primary cancer. The criteria have however been changed by cooperative groups and pharmaceutical companies to adjust to new technologies. This led to some confusion in the assessment of clinical results. In the mid-1990s, an International Working group was established to standardize the criteria. The result of this was a new set of criteria, known as RECIST (Response Evaluation Criteria in Solid Tumours), published in 2000. The main characteristic of the RECIST is that it defined the size of measurable lesions, the number of lesions to follow up and the use of unidimensional measurement of the tumor. The RECIST criteria have been recommended for image acquisition of chest X-ray, CT and MRI. This criteria are not however applicable to any functional imaging

techniques such as volumetric assessment of tumor size. Furthermore, due to poor identification of new lesions by chest radiography, the measurements of pulmonary parenchymal lesions and mediastinal disease are optimally performed with CT[43,46].

For evaluation of image quality in tomosynthesis images, no specific guidelines on quality criteria have been defined, neither in the European guidelines, nor in RECIST. Therefore, most of the studies have developed their own criteria based on the European guidelines, clinical experience and research[15,16,29,47,48].

2 AIMS OF THE THESIS

The overall aim of the studies described in this thesis was to clinically evaluate a newly developed tomosynthesis system for chest examination and its dependency on the acquisition protocol and image processing.

The aims of the separate studies were

- to evaluate the image quality of different chest tomosyntesis protocols for a newly developed tomosynthesis system by using an anthropomorphic phantom.
- to determine an optimal chest tomosynthesis protocol by evaluating the image quality based on clinical data.

Both studies are based on the Fujifilm tomosynthesis system.

3 MATERIAL AND METHODS

In this chapter, a summary of the material and methods used in paper I and II is presented.

In order to study chest tomosynthesis, a research group including one radiologist, one radiographer and one physicist was established at the department of radiology, Karolinska University Hospital.

At that time (2012), DTS technology was not used at Karolinska. The radiologist was the only team member who had clinical experience in reading chest DTS images performed and transferred from other hospitals. Prior to upgrading the system to DTS, the equipment was mostly used for conventional chest radiography examinations including postero-anterior (PA), lateral and oblique projections. The pre-defined setting for conventional chest radiography projections was with a source-to- image distance (SID) of 180 cm and automatic exposure control was 140 kV, and a total filtration of 3,5 mm Al +0,2 mm Cu.

3.1 CHEST TOMOSYNTHESIS SYSTEM

The conventional chest radiography X-ray equipment, FDR AcSelerate from Fujifilm, was originally installed for planar digital radiography imaging at the section for emergency radiology at the department of radiology, Karolinska University Hospital Solna, in October 2010. The system was equipped with a stationary CsI FPD (dimension 43 × 43 cm^2, with

resolution 2880 × 2880 pixels and a pixel size of 0.15×0.15 mm^2). In October 2012 the software and the hardware were upgraded. Additionally a reconstruction unit and a 3 Mega pixel monitor (for showing the tomosynthesis images) were installed which enabled acquisition and reconstruction of the tomosynthesis images. In 2014, the system was moved to the section of Thoracic radiology at Karolinska University Hospital, Solna due to greater interest, more clinical applications and easier/ wider availability of cancer patients at the Lung-Allergy Clinic in the same building.

Chest DTS protocols do not use the same acquisition parameter settings as conventional chest examinations. In the case of DTS protocols, for stand-up position, 10 chest DTS protocols have been defined by the vendor (Appendix 2). All projection images are acquired using a source-to-image distance (SID) of 130 or 180 cm and the tube voltage and filtration can be varied. The X-ray tube performs a continuous vertical motion and acquires 20-60 exposures in the angular interval of 10°-27° during a time period of approximately 4-12 seconds. Two different grids (with ratio 10/1 and ratio 12/1) with aluminum interspace, are used. During the vertical motion of the X-ray tube, the system produces a series of multiple exposures that are later reconstructed to tomographic slices at different depths from a single sweep of the X-ray tube. When the X-ray tube rotates around its own axis the X-ray beam passes through the pivot point and it creates a field of view (FOV), depending on SID, angle and distance between the patient and the detector (Figure 3.1).

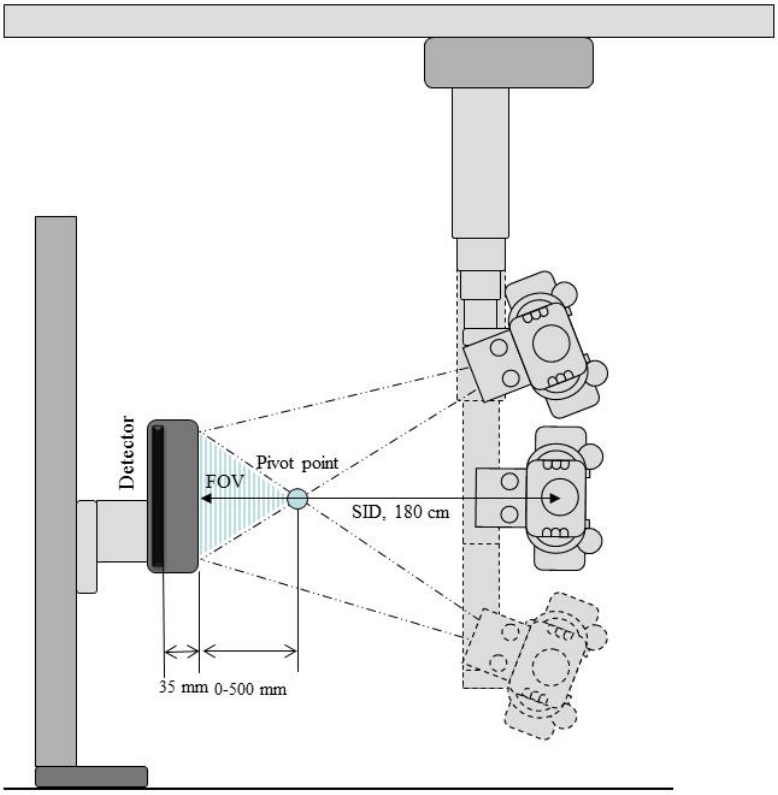

Figure 3.1. Illustration of the geometry used of the acquisition of the chest DTS projection using the FDR AcSelerate system.

When the exposure is completed, the images taken are displayed on the reconstruction unit viewer in the order they were taken (direction) and the reconstruction processing is automatically performed based on the pre-set conditions. The reconstruction processing parameters consists of center (slice height), range (slice range) and pitch (slice spacing) which are possible to alter in the reconstruction unit afterwards (Figure 3.2). There are two principles of reconstruction algorithm available in this system, shift-and-add and the vendor recommended filtered back projection (FBP). The FBP, with deblurring algorithm, has been developed by many vendors to reduce the blurred out-of- plane anatomy[16].

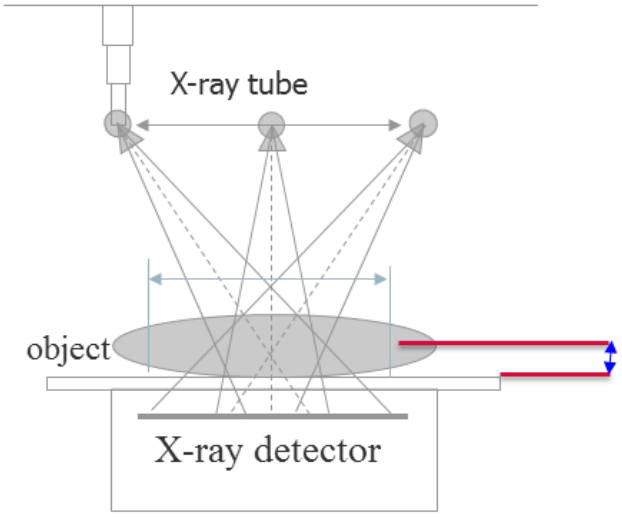

Center (slice height), distance between middle of the patient and the table/stand

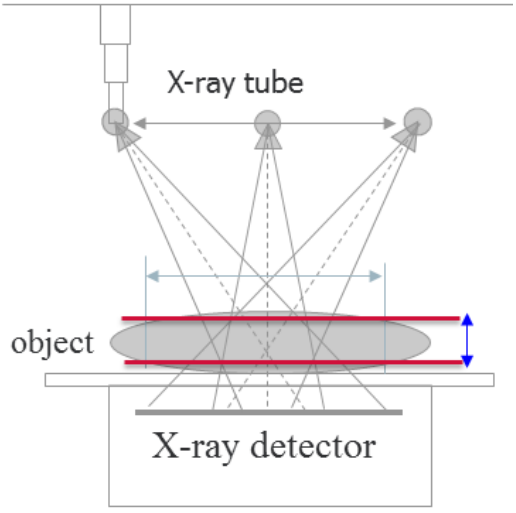

Range (slice range), the thickness of reconstruction part

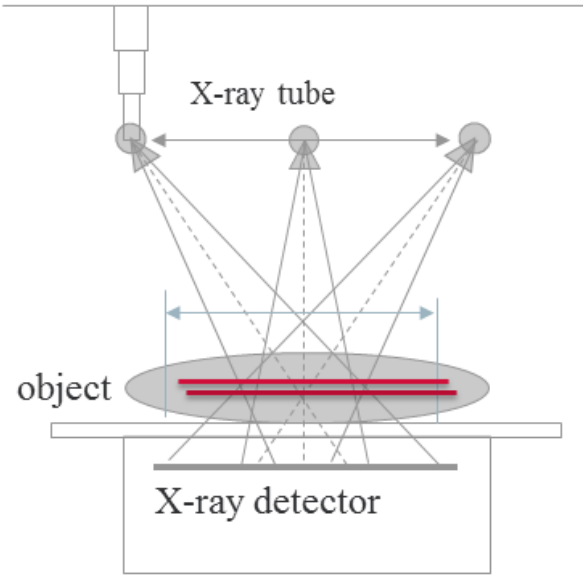

Pitch (slice spacing), distance between two slices (illustrated by the distance between the two red lines)

Figure 3.2. Definition of reconstruction processing parameters.

3.2 VISUAL GRADING METHODS

Visual grading methods are usually used for the evaluation of clinical image quality for reproduction of anatomical or pathological structures[49,50]. There are some arguments in favor of and against visual grading methods. To mention some of the pros, among others:

- The high validity of the study since the quality criteria is based on the relevant clinical structure
- In some cases the visual grading methods correspond to both methods of receiver operating characteristics (ROC) analysis and calculations of the physical image quality
- Compared to ROC, visual grading studies are relatively easy to perform, in particular while optimizing the imaging equipment
- Due to lower time consumption and workloads for each observer (radiologist), visual grading study has an economic benefit to implement at any hospital[49].

However, some of the cons that visual grading has been criticized for, is the scientific validity of the studies using this method. It is alleged that a radiologist's ability for making diagnosis is underestimated, hence the observer can select any criteria he/she finds appropriate for the image evaluation. Another criticism is the analysis of visual grading data. Given that the outcome of the grading presents in an ordinal scale, the ratings cannot be converted into numerical values[49].

Some of the common visual grading methods are image criteria (IC) and visual grading analysis (VGA). IC is based only on a two-step rating scale, where the observer indicates that a certain criterion in the image is fulfilled or not. However, in the VGA method, the observer grades the visibility of important structure by taking advantage of European quality criteria, in a multiple scales.

In VGA, there are two different methods for assessing images, the absolute rating scale and the relative rating scale. With the absolute rating scale, images are assessed one at a time, e.g. judging the visibility of a particular structure, on an absolute scale. E.g. with 5 scale steps, the lowest scale step may be presented as the number 1 and the highest scale as the number 5. A relative rating scale means the images are compared side by side with one of them being a reference image[49,51]. E.g. with 5 scale steps, the lowest scale step may be presented as the number -2 and the highest as the number +2. However, the disadvantage of VGA is that the data belongs to an ordered qualitative variable and not to a quantitative variable. This means that the differences between each scale step is not really known, for example in a case where "4" is better than "3" and "2", it is not possible to quantify how much better it is. The data from VGA study will be calculated by visual grading analysis score (VGAS) which describe the mean value of all ratings. Thus the VGAS misses the mathematical and statistical validity[15,16,23,49,50].

Due to that the calculation of common statistical values such as mean values and standard deviations is not valid for visual grading data. Båth and Månsson introduced a new method

which combines some of the strengths from both relative and absolute VGA methods, as well as IC and ROC in order to analyze the characteristics of the visual grading. This is called visual grading characteristics (VGC) analysis[49].

3.2.1 Visual grading characteristic (VGC) analysis

The main aim of developing the VGC analysis is to be able to analyze data from ordinal scales which requires non-parametric rank-invariant statistical methods. This means that the method treats the scale steps as ordinal without any assumptions about the distribution of the data being made. The VGC study can be on the basis of IC- data or VGA study, where the observer uses a multistep rating scale to determine his/her decision about the fulfillment of the image quality criteria[49,50]. The criteria are usually based on either European quality criteria or the clinical experience. The comparison can be between different acquisition settings within one image modality or between two compared modalities[16,18,49,51].

Compared with the previous visual grading methods (IC and VGA), VGC has some advantages such as:

- VGC analysis can be applied directly to the image quality criteria estabilished by the European Commission which lead to an increased validity of image quality criteria in multiple-choice grading studies.
- The VGC analysis is appropriate to use as a non-parametric rank-invariant statistical method to analyse data from an ordinal scale[49,50].

3.3 DATA COLLECTION

3.3.1 Paper I

The first study was a phantom study, for mainly two reasons. First, due to the lack of the clinical evidence for chest DTS of the FDR AcSelerate system (Fujifilm, Tokyo, Japan), a patient study was not a suitable choice. Second, in order to have a fair comparison of image quality between all DTS protocols, the same structure from the same individual should be the basis for all image evaluation. This is difficult to achieve in a patient study. With different body structures of different patients, a random variation would have entered into the study and have an effect on how good the images became. For that reason a large number of patients would have been required to get some differentiation.

A chest phantom N1 “Lungman” (Kyoto Kagaku Co. Ltd, Kyoto, Japan) with a 12 mm nodule placed in the center of the right lung was therefore used for this study.

The images were acquired using a SID of 130 or 180cm and a total filtration of 3.5mm Al 0.2mm Cu. The vertical movement of the X-ray tube acquired between 20–60 exposures in the angular interval of 10°–27° in between 4–12 s, depending on the selected protocol. Two different grids, with aluminum interspace, were used: a grid with ratio 10/1 for the focusing distance of 140cm belongs to protocols with SID 130cm and a grid with ratio 12/1 for the focusing distance of 180cm, which belongs to protocols with SID 180cm. In order to ensure an

unbiased comparison of the image quality, the tube voltage and filtration were kept constant for all protocols to achieve a constant effective dose of 0.4mSv. The phantom was placed in front of the detector (chest stand) with positioning of two markers on each side of the phantom (Figure 3.3).

Figure 3.3. Image procedure of phantom

Positioning of the markers was recommended by the vendor in order to minimize motion artifacts caused by X-ray tube vibration and to improve the reconstruction accuracy. The acquisition procedure for all 10 protocols (Appendix 2) was performed by triplicate examinations of the phantom (PA and two oblique projections) for each protocol, totaling 90 examinations for the study. In order to simulate patient variation, the position of the phantom had been changed by different angulation of oblique projections, within triplicate examinations for each protocol. During the exposure, the X-ray tube had a linear movement from down to up, while the detector was fixed. After reconstruction of the images in the reconstruction unit, the images were transferred to the picture archiving and communication system (PACS) (Sectra Medical Systems, Linköping, Sweden) for further evaluation.

3.3.2 Paper II

Based on the result from the anthropomorphic phantom study, a patient study was planned to evaluate the image quality of two DTS protocols based on the acquisition settings and image post-processing. As the result of the first study was that the ID 65 with an exposure time of 6.3 s was the only DTS protocol with similar quality as the vendor recommended protocol, ID 76 with 12 s. exposure time, for all classes of criteria, it was decided to do a second study to compare only those two protocols in a clinical trial. This clinical study would provide formal evidence of the comparison between the vendor-recommended protocol and a protocol with half of the acquisition time, crucial for some of the cancer patients with dyspnea. In addition, small movements during exposure is detrimental to the quality of reconstructed images, which also makes shorter acquisition time attractive.

Between August 2014 and May 2015, a total number of 20 patients (12 males and 8 females) with suspected pulmonary malignancies, who had been referred to the Lung-Allergy Clinic at Karolinska University Hospital, were scheduled for DTS examination. In order to compare the image quality of those two protocols ID 65 and ID 76 (appendix 2)[15], it required two DTS examinations in postero-anterior direction in upright position for each patient (Figure 3.4). The acquisitions were performed in a random order.

Figure 3.4. A chest tomosynthesis examination in the Posterior Anterior (PA) position. Information was derived from Fujifilm, Tokyo, Japan.

For both protocols the vendor recommended tomosynthesis setting, the tube voltage and filtration were kept constant. However, the tube current (mA) was modified for each protocol in order to keep a constant effective dose of 0.4 mSv for both protocols[16,19]. The patient was clearly informed to hold his/her breath during each acquisition. Due to the requirement of the exchange of the grid between two acquisitions, the patient had time to rest for approximately 4 minutes. For each patient, two DTS series with acquisition time of 6.3 and 12 s were performed. During exposure the detector was fixed while the X-ray tube rotated linearly in the α-direction. Afterwards, both series (ID 65 and 76) were processed using the vendor recommended image processing parameter, as gradation processing but also as a separate series with additional image parameters, such as MFP and FNC. MFP and FNC image parameters has been used clinically for conventional chest radiography at the Radiology department at Karolinska University hospital, Solna. The four sets of reconstructed images per patient were transferred to PACS system (Sectra Medical Systems, Linköping, Sweden).

3.4 DATA EVALUATION

In the first study in this thesis, the relative visual grading was used. However, in order to rate image quality, numerical values were used which represented an ordinal scale. As a result, the ratings were treated as ordinal data in the statistical analysis. In addition, since the ratings were made based on the comparison with one and the same protocol, evaluated by all observers, they could statistically be treated as absolute and allowing the application of VGC analysis. However, in the second study, the absolute visual grading was used as the images were evaluated one by one[15,16].

Both studies were based on multi-step scale rating (five scale steps ranging) from "image quality much lower than in the comparison protocol" (-2) to "image quality much higher than in the comparison protocol" (+2) (for paper I) and "very bad" to "very good" (for paper II)[15,16]. The result of the multi-step scale rating is a VGC curve which is created by plotting the accrued proportion of ratings above a certain threshold for a tested imaging condition compared with the same proportion for a reference condition. The differentiation between those two tested conditions is presented by a figure merit i.e. the area under VGC curve (AUC_{VGC}) (Figure 3.5)[16,48,50,51].

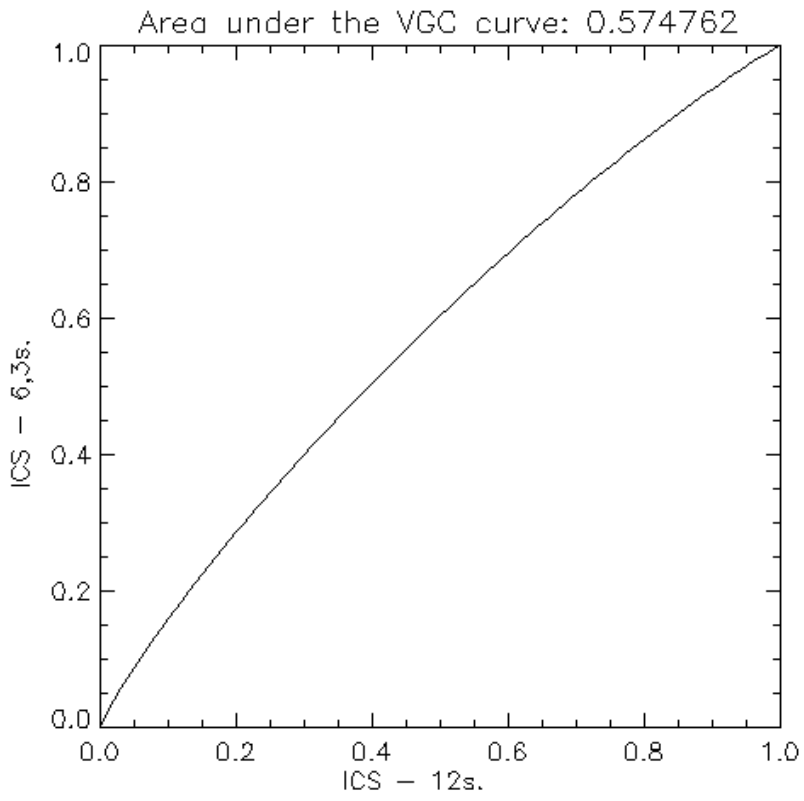

Figure 3.5. An example of a visual grading characteristics curve, reflecting how the proportion of images that are judged as being of higher quality than a certain threshold for protocol identity ID 65 (with acquisition times 6.3 s) varies with this proportion for protocol ID 76 (with acquisition times 12 s), when the threshold is altered, for the disturbance class of criteria.

A VGC curve from the data ranges from 0.0 to 1.0 and the deviation of the curve from the diagonal indicates the difference in image quality between the two compared settings or techniques. With an AUC_{VGC} of or near 0.5 it can be considered that the two systems or settings produce identical image quality. However, an $AUC_{VGC} < 0.5$ indicates better image quality for the reference image/system and an $AUC_{VGC} > 0.5$ indicates better image quality for the evaluated image/system. The difference from an AUC_{VGC} of 0.5 can be used for significance testing[18,48].

Due to the lack of national as well as international guidelines on quality criteria for diagnostic chest DTS images, the criteria used in both studies were developed based on the European guidelines for diagnostic radiographic[44] and CT images[45], as well as the criteria for DTS proposed by Asplund et al, complemented by the clinical experience of the research team[47]. The criteria for both studies are listed, in Appendix 3[15] and Appendix 4[16].

3.4.1 Paper I

Four senior consultant radiologists, each with more than two decades of experience with chest diagnostics, assessed the DTS images based on four classes of criteria, (demarcation, disturbance, structure and homogeneity in the nodule) on the PACS workstation (Appendix 3). The criteria covered eight anatomical regions with different types of structures, each marked with a letter (A-H) on the image as starting point for evaluation of that particular region (Figure 3.6)[15].

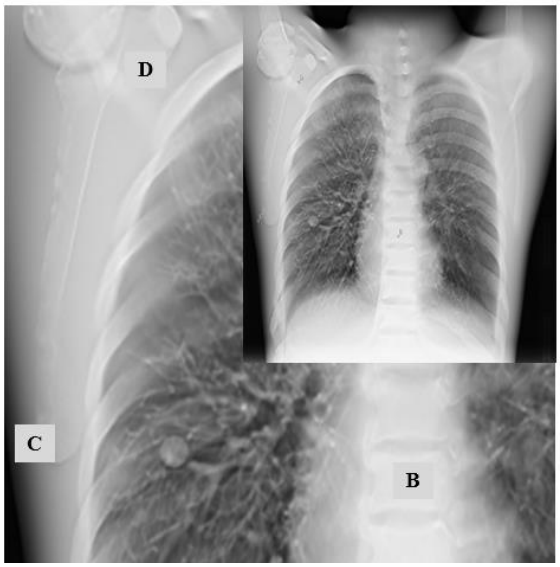

Figure 3.6. Three example of the anatomical regions: B, lower thoracic spine; C, peripheral vessels approximately 1mm and D, vessels around the inserted nodule approximately 3mm.

Due to statistical reasons, the images acquired with protocol ID 70 were selected as comparison images in the relative grading evaluation, meaning that the images were compared side by side. It was assumed that the image quality acquired from this protocol would be adequate to use for the entire rating scale. Therefore the protocol ID 70 was rated as "0" related to all criteria. The DTS series of images were displayed in a random order and were identified by a code unrelated

to the type of the protocol. The series of DTS images to be assessed, were displayed on the left screen and the corresponding series of images from protocol ID 70 on the right screen, thus paired in order to ensure the same projection level. For each comparison, the image quality related to each criteria was rated on a five-step scale from "image quality much lower than for the comparison protocol" (-2) to "image quality much higher than for the comparison protocol" (+2).

In the VGC analysis, the vendor recommended protocol ID 76 was used as the reference. By using the VGC Analyzer (in-house developed software, University of Gothenburg, Gothenburg, Sweden)[52,53] for each class of criteria, a VGC curve averaged over observers' results was determined and the asymmetric 95% confidence interval of the area under the VGC curve (AUC_{VGC}) was determined by a bootstrapping (resampling) method.

3.4.2 Paper II

For the evaluation of the image quality of the reconstructed DTS series, a DICOM image viewer software, ViewDEX, developed at Sahlgrenska University Hospital, Gothenburg, Sweden, was used [54-56]. Four senior consultants individually assessed the image quality blinded and in a unique random order, conducted automatically by ViewDEX DICOM reader software, on the same display, and the result was stored automatically in a log file for analysis. The evaluation of the image series was managed on a Mac Book pro, 15" Retina display with a 2880 x 1800 resolution, with two graphics cards, each powerful enough to utilize the high-resolution display. Compared to the first study (relative visual grading), an absolute visual grading was used in this study, meaning that the image series in this study were evaluated one at a time on an absolute scale. Similar to the previous study, the criteria focused on the image quality in pre-determined anatomical regions. All observers assessed the image quality in five different anatomical regions and rated the image quality related to each criterion on a 5-step ordinal scale; (1) very bad, (2) bad, (3) fair, (4) good and (5) very good. The identification of the images was done by a code unrelated to the type of protocol ID and post processing parameters.

In comparison between the protocol ID 65 with an acquisition time of 6.3 s and a vendor recommended protocol ID 76 with an acquisition time of 12.0 s as reference for VGC analysis, the AUC_{VGC} and p-values for each class of criteria and the type of post processing were calculated.

The data were analysed by the VGC method in two types of VGC analyses. One analysis was for comparing the two acquisition protocols, ID 65 and ID 76. In this case the ID 76 was used as the reference protocol and ID 65 as the test protocol. In the second analysis, the vendor recommended post processing for DTS (GP) was used as the reference, and the MFP/FNC parameters as the test. The observers scored the image quality based on three classes of criteria: demarcation, disturbance and structure (appendix 4)[16].

3.5 ETHICAL CONSIDERATION

For the first study, no ethical approval was needed, as it did not involve any patient for data collection. However, ethical approval had been taken into account for the second study and approval from Regional Ethical Review Board in Stockholm was obtained (reference number: 2012/1198-31/1 and 2013/1074-32). Patients had to be a minimum of 18 years old to be included in the study. The first application was intended for only 10 patients, whereas the second application was submitted to include 20 patients in the study. According to Karolinska university Hospital regulations, a permit from the Radiation Protection Committee was required (reference number K2166-2013). Furthermore, signed informed patient consent was received from all participants.

Independent studies have presented the potential role of chest tomosynthesis compared with chest radiography (CXR) and CT for nodule detection and detection of pulmonary metastases in thoracic radiology[3,12,43,57,58]. However, there is still a need for scientific evidence and clinical expertise on the DTS modalities. Even though the 20 patients did not benefit themselves from the two additional DTS acquisitions, the result of this study can be beneficial for patients in the future. This justifies the small additional radiation dose to the patients in this study.

4 RESULTS

In this chapter, an overview of the results of studies presented in Papers I and II is given.

4.1 PAPER I

In comparison with the protocol ID 76 as reference for VGC analysis, the AUC_{VGC} and p-values for nine chest DTS protocols and each class of criteria were calculated (Table 4.1)[15].

Table 4.1 AUC_{VGC} and p-values for the different chest DTS protocols and the four classes of quality criteria.

DTS exposure ID		**Demarcation**		**Disturbance**		**Structure**		**Homogeneity in nodule**	
	Tube swing angle (°)	AUC_{VGC}	P-value	AUC_{VGC}	P-value	AUC_{VGC}	P-value	AUC_{VGC}	P-value
60	10	0.58	n.s.	0.05	< 0.001	0.70	< 0.01	0.14	< 0.01
61	13	0.42	n.s.	0.12	< 0.001	0.62	< 0.05	0.24	< 0.05
62	15	0.38	< 0.05	0.20	< 0.001	0.59	n.s.	0.33	0.05
65	20	0.44	n.s.	0.34	n.s.	0.53	n.s.	0.45	n.s.
66	25	0.39	< 0.05	0.43	n.s.	0.44	n.s.	0.52	n.s.
70	10	0.59	n.s.	0.03	< 0.001	0.74	< 0.05	0.00	< 0.01
71	14	0.55	n.s.	0.10	< 0.001	0.70	< 0.01	0.28	0.05
73	15	0.57	n.s.	0.22	< 0.01	0.68	0.05	0.33	n.s.
74	20	0.54	n.s.	0.27	< 0.01	0.50	n.s.	0.38	n.s.

As shown in the table above, the protocols with a smaller swing angle resulted in lower image quality for the classes of criteria such as “disturbance” and “homogeneity in nodule”. The same swing angle did however result in a higher image quality for the “structure” class of criteria. The class of criteria “demarcation” presented a small dependency on the swing angle. ID 65 was the only DTS protocol which showed no significant difference from the reference protocol ID 76 for any class of criteria. The benefit of protocol ID 65 was that it has a shorter exposure

time 6.3 s vs the vendor recommended protocol ID 76 which has 12 s. All other protocols showed significantly lower image quality than the reference protocol.

Another aspect of the comparison was SID. For the class of criteria "demarcation", the protocol IDs 62 and 66 with 130 cm scored a lower image quality compared with the reference protocol. In comparison, the protocols with SID 180 cm yielded similar quality as the reference protocol for same class of criteria. All protocols with SID of 180 cm led to significantly lower image quality than the reference protocol for the class of criteria "disturbance". However, the protocol IDs 65 and 66 with a SID 130 cm showed similar image quality for "demarcation" as the reference protocol.

For the "structure" and "homogeneity in nodule" class of criteria, there was no proof of dependency on the SID.

4.2 PAPER II

The result of the VGC analysis presented a small but statistically significant advantage for the protocol ID 65 over the protocol ID 76 for both the classes of criteria "demarcation" (AUC_{VGC} = 0.56, p = 0.009) and "disturbance" (AUC_{VGC} = 0.58, p < 0.001). For the class of criteria "structure" a similar value of AUC_{VGC} was found. However, the difference was not statistically significant (AUC_{VGC} = 0.56, p = 0.21).

Regarding the two types of post processing, the vendor recommended standard GP processing (as reference for VGC analysis) and GP/MFP/FNC, the VGC analysis represented a small but statistically significant advantage for the GP processing over the other, that included more processing, for the classes of criteria "demarcation" (AUC_{VGC} = 0.45, p = 0.017) and disturbance (AUC_{VGC} = 0.43, p = 0.005). For the class of criteria "structure" a similar value of AUC_{VGC} was found. However, the difference was not statistically significant (AUC_{VGC} = 0.46, p = 0.31).

5 DISCUSSION

The main aim of this thesis was to investigate the effect of different image acquisition parameters and post processing parameters in the chest DTS by assessing image quality in predetermined anatomical regions. The evaluation was based on predetermined quality criteria. Furthermore, the thesis aimed to determine a chest DTS protocol with a shorter exposure time than the vendor-recommended protocol (12 s), while retaining image quality. Such a protocol would have clinical advantages for patients with conditions such as thoracic malignancy, as movement during exposure degrades the image quality. This was investigated by examining a number of alternative predefined chest DTS protocols in a phantom study. From this initial study, a protocol with a shorter acquisition time (6.3 s) but with an equal image quality as the vendor-recommended protocol (12 s) was selected. The selected protocol was tested via a group of patients with suspected lung cancer and compared with images from the protocol recommended by the vendor. In addition to the comparison of image quality based on acquisition time, two other types of image processing parameters were compared as well. It was found that the tested protocol with an acquisition time of 6.3 s yielded better image quality than the vendor recommended protocol with an acquisition time of 12 s for several anatomical structures. At the same time, the vendor-recommended image processing parameters provided a certain advantage over MFP-FNC processing.

As described by Båth et al.[59], this thesis has followed an optimization strategy of new technology in a digital environment. The authors summarized the optimization strategy in three steps, 1) the optimization of images should be based on anthropomorphic phantom or clinical images; 2) all comparisons should be performed at equal effective dose. 3) The optimization process will start with determining the optimal parameter setting of the system, followed by selecting the optimal image viewer and finally, keeping the radiation dose as low as possible while obtaining acceptable image quality. It is important to note, that it is advised to always include the anatomical background during the optimization[59]. Paper I reflected on the first and the second steps. Paper II corresponds to the third optimization step, in this case specifically on determining the DTS protocol and post processing parameters with maintained image quality. In addition, both studies in this thesis follow the proposal of Båth et al. to include anatomical background in the optimization process.

In a similar study as that presented in Paper I, Söderman et al.[48] evaluated the quality of chest DTS images using the GE tomosynthesis system. An anthropomorphic phantom was scanned by nine different projection image configurations (incl. default setting) while each configuration acquired with ten different tube voltages, in the range between 60kVp to 150kVp in steps of 10 kVp. The system configurations were evaluated based on the number of project images, respectively, from 15 to 60 and the sweep angle, respectively, from 7.5° to 30°. For all system configurations the total effective dose was kept constant and 65 section images were reconstructed at 5 mm intervals. Four thoracic radiologists participated in a visual grading study. The image quality criteria related to the reproduction of the trachea, of the small, medium and large sized vessels, of the paratracheal tissue, of the thoracic aorta and clinically acceptable

artifacts, were included. The criteria were based on the anatomical structures proposed in the previous study by Asplund et al[47]. For evaluation of the data, VGC analysis was used and the vender-recommended configuration, which included 60 projection images and an sweep angel of 30° and a projection image density of 2.0/° was used as reference in the analysis. The results related to the effect of the angular interval on the image quality, were similar to what was reported in Paper 1. The configurations with the smallest sweep angel (7.5°, 10°, and 15°) shown a significantly lower image quality than the vendor-recommended configuration for the criteria related to follow vessels through the volume. However, Söderman et al. did not evaluate the visibility of spine, but instead of that, a criterion, "*Clear reproduction of the trachea*" was included. For this criterion, the images quality increased with decreasing sweep interval. Regarding the tube voltage, Söderman identified that no alternative tube voltage did have a large impact on the image quality than the vendor- recommended settings (120kVp) for any criterion. The conclusion was that the default configuration for chest DTS consisting of 60 projection images acquired by 30° sweep angel is a good option.

In concordance with the Paper I and II, and the results given by Söderman et al.[48] considered above, Machida et al.[20] emphasized the importance of the acquisition parameters for obtaining high quality of the DTS images while decreasing artifacts and keeping the radiation dose as low as reasonably achievable (ALARA). The most important parameters of DTS protocols that should be optimized are sweep angle, sweep direction, SDD, number of projection images and total radiation exposure. Thus, it was concluded that it is essential to determine the appropriate protocols for different anatomical areas in order to utilize DTS imaging technique.

Previous studies have shown the potential role of chest tomosynthesis in replacing CXR and CT examinations or as an addition to these examinations for some patient group[3,11,23,58]. Petersson et al. presented that DTS can substitute CXR and chest CT modalities during office hours by 20% and 25%, respectively, and that CT would be the option of 63% of chest DTS if DTS modality was not available[58]. Other studies concluded that DTS is a better alternative for detectability of nodules compare with CXR[3,11,60] and that DTS can be an option instead of CT for detection of artificial nodules[61] and metastases from colorectal cancer[43].

In a study similar to that in paper II, Meltzer et al.[62] evaluated the quality of chest DTS images, using a GE imaging system. 21 patients with cystic fibrosis were identified by anatomical structures in predefined regions based on CT images for comparison of visibility with DTS images. These regions of the lungs were selected, because it was already known to be a problem when using DTS. Four anatomical levels were selected which covered different parts of the lung parenchyma (lung lobes). The visibility of structures in the DTS images was evaluated with the corresponding structure in CT images. The result, based on 30 predefined anatomical structures which were evaluated by three observers, was presented as equal to CT in 34% of cases, inferior in 52% and superior in 14%. In general, structures in central and peripheral lateral areas obtained higher visibility with DTS compared with peripheral structures anteriorly, posteriorly and surrounding the diaphragm. Similar to the studies in this thesis, they designed their study in order to evaluate the depth resolution and motion artefacts. The authors found the

problem with depth resolution in the areas of parenchymal structures next to high dense area such as clavicle, ribs, sternum, large vessels, heart and diaphragm. The motion artifacts were visible around the diaphragm. In contrast to the Meltzer study, no motion artifacts could be seen in the patient study in this thesis. Meltzer concluded that due to DTS limitations in providing visibility to minor pathology, further research is required to look into the clinical importance of tomosynthesis.

Paper I has a number of limitations. First the initial phantom study does not really reflect the conditions for patients where a number of other factors influence image quality, e.g. patient size and movement. However, it would not have been ethical to compare 9 protocols and perform 9 examinations on each subject. To perform only one DTS protocol per patient and then make comparisons on a group level would have required large groups to allow for reliable statistics. Hence, this "two stage rocket" approach was the only alternative. The second limitation is that some of the observers did not have enough experience in DTS image reading. However, they did have more than 20 years' experience in radiology. All observers had access to a learning section before they performed the real evaluation, in order to compensate for the lack in experience.

Paper II also has some limitations. The main limitation is the limited number of patients. This is mainly due to concerns for radiation protection. Also, collecting patient data is logistically challenging and our resources were limited. The second limitation is lack of a quality criterion for assessing the depth resolution, although the disturbance class of criteria will be effected of depth resolution. The third limitation is that the evaluation of DTS images was performed on a laptop, Mac Book Pro instead of in a PACS workstation. Due to different geographic location of the observers, the images were transferred to an external laptop making the images accessible for all observers. The monitor's image quality was however compared with the PACS workstation and approved by an experienced thoracic radiologist. The fourth limitation is due to clinical evaluation of only two DTS protocols from paper I. However, performance of all protocols in a clinical trial would not have been ethical.

The common limitation for both studies, is the lack of international guidelines on quality criteria for DTS image reading. Given the fact that, the European guidelines do not cover the quality criteria for DTS and also that there is a shortage of studies evaluating the anatomical structures throughout chest, the image quality criteria were developed based on the criteria suggested by Asplund[47] together with the existing European guidelines on quality criteria for radiographic[44] and CT images[45].

In conclusion this thesis indicates that a shorter acquisition time may be clinically relevant, and in some cases essential for patients with respiratory failure.

6 FUTURE PERSPECTIVES

Until today, most DTS studies have been based on the comparison between chest DTS and two other modalities, CXR and CT, to investigate the detectability of lung nodules. However, the radiation dose for all three modalities has always been an essential parameter in obtaining reliable chest image quality. Asplund et al. found in 2014[63] that it is possible to reduce the radiation dose significantly from the default setting of the GE DTS system. For study purposes, an additional DTS examination was performed in addition to the scheduled chest CT examination of 86 patients. The majority of the patients had a known malignant disease including lung cancer, breast cancer, head and neck cancer and lymphoma. By adding artificial noise, the DTS images were generated similar to a reduction by 12%, 32% and 70% of the default effective dose (0.12 mSv). The result showed that the standard of nodule detectability remained even when the dose was reduced by 32%. The conclusion therefore is that the dose reduction for a chest DTS examination can be of value, if it enables the inclusion/acceptance of chest tomosynthesis as a standard method for detecting lung nodules and other lung diseases. This also leads to a reduced patient exposure.

Some lung diseases, pulmonary nodules for example, require further investigation with PET or PET-CT in addition to CXR and CT, within a short period of time[38,64]. In these cases, tomosynthesis can be an alternative for follow-up after CT and PET in order to reduce cost and radiation dose to patients who have already gone through several high radiation dose examinations. Normally, at Karolinska University hospital, the follow up cases, where accidental nodules have been detected, require up to 4 chest CT examinations, before follow up can be stopped. This is in accordance with recommendations from the American Thoracic Society[65]. Tomosynthesis could be an option to replace at least two of the chest CT exams, with the CT and PET-CT used as reference image. Further clinical studies are however, required to evaluate the reliability of chest DTS compared to CT and CXR. In addition to optimizing the DTS protocol parameters for lung nodule detection, the use of chest DTS should be evaluated for different diagnostic questions and potentially as a replacement for chest screening programs instead of CT. Apart from the diagnostic value of modalities, radiation exposure, examination time and cost should be evaluated. Due to CXR and DTS being performed in the same system, it makes DTS modalities easy to use, inexpensive and accessible in comparison to a CT and PET/PET-CT combination. By optimizing the workflow and examination procedure between different modalities, chest DTS will not only add clinical value to image quality, but can even contribute to the reduction of patient exposure. These benefits will in turn lead to cost efficiencies within healthcare.

7 REFERENCES

1. McAdams HP, Samei E, Dobbins JT, Tourassi GD, Ravin CE. Recent advances in chest radiography. Radiology 2006; 241: 663–83.
2. Zhang Y, Li X, Segars WP, Samei E. Comparison of patient specific dose metrics between chest radiography, tomosynthesis, and CT for adult patients of wide ranging body habitus. Med Phys 2014; 41: 023901.
3. Vikgren J, Zachrisson S, Svalkvist A, Johnsson AA, Boijsen M, Flinck A, et al. Comparison of chest tomosynthesis and chest radiography for detection of pulmonary nodules: human observer study of clinical cases. Radiology 2008; 249: 1034–41.
4. Galea A, Adlan T, Gay D, Roobottom C, Dubbins P, Riordan R. Comparison of digital tomosynthesis and chest radiography for the detection of noncalcified pulmonary and hilar lesions. J Thorac Imaging 2015; 30: 328-35.
5. Brenner DJ, Hall EJ. Computed tomography- An increasing source of radiation exposure. N Engl J Med 2007; 357: 2277-84.
6. Dobbins JT, McAdams HP. Chest tomosynthesis: Technical principles and clinical update. Eur J Radiol 2009; 72: 244-51.
7. Wolbarst AB, Hendee WR. Evolving and experimental technologies in medical imaging. Radiology 2006; 238: 16-39.
8. Johansen A, Conners GP, Lee J, Robinson AL, Chew WL, Chan SS. Pediatric Esophageal Foreign Body: possible Role for digital tomosynthesis. Pediatr Emerg Care 2018; 29768297.
9. Båth M, Håkansson M, Börjesson S, Kheddache S, Grahn A, François O, et al. Nodule detection in digital chest radiography: Part of image background acting as pure noise. Radiat Prot Dosimetry 2005; 114: 102-8.
10. Yamada Y, Shiomi E, Hashimoto M, Abe T, Matsusako M, Saida Y, Ogawa K. Value of a computer- aided detection system based on chest tomosynthesis imaging for the detection of pulmonary nodules. Radiology 2018; 287: 333-39.
11. Yamada Y, Jinzaki M, Hasegawa I, Shiomi E, Sugiura H, Abe T, et al. Fast scanning tomosynthesis for the detection of pulmonary nodules: diagnostic performance compared with chest radiography, using multidetector-row computed tomography as the reference. Invest Radiol 2011; 46: 471-7.
12. Dobbins JT, McAdams HP, Song JW, Li C, Godfrey DJ, DeLong DM, et al. Digital tomosynthesis of the chest for lung nodule detection: interim sensitivity results from an ongoing NIH-sponsored trial. Med Phys 2008; 35: 2554–57.
13. Lee XW, Marshall HM, Leong SC, Rourke RL, Steinke K, Mirjalili N, et al. Is digital tomosynthesis on par with computed tomography for the detection and measurement of pulmonary Nodules? J Thorac Imaging 2017; 32: 67-68.
14. Meltzer C, Vikgren J, Bergman B, Molnar D, Norrlund RR, Hassoun A, et al. Detection and characterization of solid pulmonary nodules at digital chest tomosynthesis:Data from a cohort of the pilot Swedish cardiopulmonary bioimage study. Radiology 2018; 287: 1018-27.

15. Jadidi M, Sundin A, Aspelin P, Båth M, Nyrén S. Evaluation of a new system for chest tomosynthesis: aspects of image quality of different protocols determined using an anthropomorphic phantom. Br J Radiol 2015; 88: 20150057.
16. Jadidi M, Båth M, Nyrén S. Dependency of image quality on acquisition protocol and image processing in chest tomosynthesis - A visual grading study based on clinical data. Br J Radiol 2018; 91: 20170683.
17. Sabol JM. A Monte Carlo estimation of effective dose in chest tomosynthesis. Med Phys 2009; 26: 5480–7.
18. Båth M, Svalkvist A, von Wrangel A, Rismyhr-Olsson H, Cederblad A. Effective dose to patients from chest examinations with tomosynthesis. Radiat Prot Dosimetry 2010; 139: 153–58.
19. Svalkvist A, Mansson LG, Bath M. Monte Carlo simulations of the dosimetry of chest tomosynthesis. Radiat Prot Dosimetry 2010; 139: 144–52.
20. Machida H, Yuhara T, Mori T, Ueno E, Moribe Y, Sabol JM. Optimizing parameters for flat-panel detector digital tomosynthesis. Radiographics 2010; 30: 549–62.
21. Svalkvist A. Development of methods for evaluation and optimization of chest tomosynthesis. 1 ed. Gothenburg: Geson Hylte tryck AB; 2011.
22. Dobbins JT, Ravin CE, Tomosynthesis imaging: At a translational Crossroads. Med Phys 2009; 36: 1956-67.
23. Asplund S. Detection of pulmonary nodules in chest tomosynthesis. Comparision with chest radiography, evaluation of learning effects and investigation of radiation dose level dependency. 1 ed. Gothenburg: Aidla Trading AB; 2014.
24. Garrison JB, Grant DG, Guier WH, Johns RJ. Three dimmensional roentgenography. AJR 1969; 105: 903-8.
25. Dobbins JT, Godfrey DJ. Digital X-ray tomosynthesis: current state of the art and clinical potential. Phys Med Biol 2003; 48: R65-R106.
26. Ziegler CM, Franetzki M, Denig T, Mühling J, Hassfeld S. Digital tomosynthesis-experiences with a new device for the dental field. Clin Oral Invest 2003; 7: 41-45.
27. Spahn M. Flat detectors and their clinical applications. Eur Radiol 2005; 15: 1934-47.
28. Johnsson Å A, Vikgren J, Bath M. Chest tomosynthesis: technical and clinical perspectives. Semin Respir Crit Care Med 2014; 35: 17–26.
29. Berggren K, Cederström B, Lundqvist M, Fredenberg E. Technical Note: Comparison of first- and second-generation photon-counting slit-scanning tomosynthesis systems. Med Phys 2018; 45: 635-38.
30. Seibert JA. Flat-panel detectors: how much better are they? Pediatr Radiol 2006; 36: 173-81.
31. Yamada S, Murase K. Effectiveness of flexiblenoise control image processing for digital portal images using computed radiography. Br J Radiol 2005; 78: 519–27.
32. Fuji Photo Film Co., LTD. FCR (Fuji Computed Radiography) general description of image processing. Tokyo, Japan: Fujifilm I&I- Imaging & Information; 2002.
33. Freedman MT, Artz DS. Digital Radiography of the chest. Semin Roentgenol 1997; 32: 38-44.

34. Horva´th A´, Wolf P, Nagy J, Kelemen A, Horva´th G, Dadh a´zi D, et al. Overview of a digital tomosynthesis development: new approaches for low-dose chest imaging. Radiat Prot Dosimetry 2016; 169: 171-6.
35. Barta JA, Powell CA, Wisnivesky JP. Global epidemiology of lung cancer. Ann Glob Health 2019; 85: 30741509.
36. Kruamak T, Edwards R, Cheng S, Hippe DS, Raghu G, Pipavath SNJ. Accuracy of digital tomosynthesis of the chest in detection of interstitial lung disease comparison with digital chest radiography. J Comput Assist Tomogr 2018; 43: 109-14.
37. Kim EY, Chung MJ, Lee HY, Koh WJ, Jung HN, Lee KS. Pulmonary mycobacterial disease: diagnostic performance of low-dose digital tomosynthesis as compared with chest radiography. Radiology 2010; 257: 269-277.
38. Gould MK, Lillington GA. Strategy and cost in investigating solitary pulmonary nodules. Thorax 1998; 53: 32–7.
39. Diederich S, Das M. Solitary pulmonary nodule: detection and management. Cancer Imaging 2006; 6: 42–6.
40. Quaia E, Baratella E, Cioffi V, Bregant P, Cernic S, Cuttin R, et al. The value of digital tomosynthesis in the diagnosis of suspected pulmonary lesions on chest radiography: analysis of diagnostic accuracy and confidence. Acad Radiol 2010; 17: 1267-74.
41. Quaia E, Baratella E, Poillucci G, Kus S, Cioffi V, Cova MA. Digital tomosynthesis as a problem-solving imaging technique to confirm or exclude potential thorscic lesions based on chest x-ray radiography. Acad Radiol 2013; 20: 546-553.
42. Lee G, Jeong YJ, Kim KI, Song JW, Kang DM, Kim YD, et al. Comparison of chest digital tomosynthesis and chest radiography for detection of asbestos-related pleuropulmonary disease. Clin Radiol 2013; 68: 376-82.
43. Jung HN, Chung MJ, Koo JH, Kim HC, Lee KS. Digital tomosynthesis of the chest: Utility for detection of lung metastasis in patients with colorectal cancer. Clin Radiol 2012; 67: 232-38.
44. CEC. European guidelines on quality criteria for diagnostic radiographic images. Report EUR 16260 EN. Luxembourg: Office for Official Publications of the European Communities; 1996.
45. CEC. European guidelines on quality criteria for computed tomography. Report EUR 16262 EN. Luxembourg: Office for Official Publications of the European Communities; 1996.
46. Eisenhauer EA, Therasse P, Bogaerts J, Schwartz LH, Sargent D, Ford R, et al. New response evaluation criteria in solid tumours: revised RECIST guideline (version1.1). Eur J Cancer 2009; 45: 228-247.
47. Asplund S, Johnsson ÅA, Vikgren J, Svalkvist A, Boijsen M, Fisichella V, et al. Learning aspects and potential pitfalls regarding detection of pulmonary nodules in chest tomosynthesis and proposed related quality criteria. Acta Radiol 2011; 52: 503–12.
48. Söderman C, Asplund S, Allansdotter Johnsson Å, Vikgren J, Rossi Norrlund R, Molnar D, et al. Image Quality dependency on system configuration and tube voltage in chest

tomosynthesis- a visual grading study using an anthropomorphic chest phantom. Med Phys 2015; 42 :1200-12.
49. Båth M, Månsson LG. Visual grading characteristics (VGC) analysis: a non-parametric rank-invariant statistical method for image quality evaluation. Br J Radiol 2007; 80: 169-76.
50. Ludewig E, Richter A, Frame M. Diagnostic imaging- evaluation image quality using visual characteristic (VGC) analysis. Vet Res Commun 2010; 34: 473-79.
51. Söderman C. Optimization of image acquisition parameters in chest tomosynthesis. Experimental studies on pulmonary nodule assessment and perceived image quality. Sahlgrenska Academy, institute of clinical sciences. Gothenburg, Sweden; 2016.
52. Båth M, Hansson J. VGC analyzer: a software for statistical analysis of fully crossed multiple reader multiple-case visual grading characteristics studies. Radiat Prot Dosimetry 2016; 169: 46–53.
53. Hansson J, Månsson LG, Båth M. The validity of using ROC software for analyzing visul grading characteristics data: an investigation based on the novel software VGC analyzer. Radiat Prot Dosimetry 2016; 169: 54–9.
54. Börjesson S, Håkansson M, Båth M, Kheddache S, Svensson S, Tingberg A, et al. A software tool for increased efficiency in observer performance studies in radiology. Radiat Prot Dosimetry 2005; 114: 45–52.
55. Håkansson M, Svensson S, Zachrisson S, Svalkvist A, Båth M, Mansson LG. ViewDEX: an efficient and easy-to-use software for observer performance studies. Radiat Prot Dosimetry 2010; 139: 42–51.
56. Svalkvist A, Svensson S, Håkansson M, Båth M, Mansson LG. ViewDex: a status report. Radiat Prot Dosimetry 2016;169: 38–45.
57. Lee KH, Goo JM, Lee SM, Park CM, Bahn YE, Kim H, et al. Digital tomosynthesis for evaluating metastatic lung nodules: nodule visibility, learning curves, and reading times. Korean J. Radiol. 2015; 16: 430-39.
58. Petersson C, Båth M, Vikgren J, Allansdotter Johnsson Å. An analysis of the potential role of chest tomosynthesis in optimizing imaging resources in thoracic radiology. Radiat Prot Dosimetry 2016; 169: 165-170.
59. Båth M, Håkansson M, Hansson J, Månsson LG. A conceptual optimisation strategy for radiography in a digital environment. Radiat Prot Dosimetry 2005; 114: 230-35.
60. Kim SM, Chung MJ, Lee KS, Kang H, Song IY, Lee EJ et al. Digital tomosynthesis of the thorax: the influence of respiratory motion artifacts on lung nodule detection. Acta Radiol 2013; 54: 634-39.
61. Gomi T, Nakajima M, Fujiwara H, Takeda T, Saito K, Umeda T, et al. Comparision between chest digital tomosynthesis and CT as ascreening method to detect artificial pulmonary nodules: a phantom study. Br J Radiol 2012; 85: 622-29.
62. Meltzer C, Båth M, Kheddache S, A´sgeirsdo´ttir H, Gilljam M, Allansdotter Johnsson Å. Visibility of structures of relevance for patients with cystic fibrosis in chest tomosynthesis: influence of anatomical location and observer experience. Radiat Prot Dosimetry 2016; 169: 177-87.

63. Asplund SA, Johnsson ÅA, Vikgren J, Svalkvist A, Flinck A, Boijsen M, et al. Effect of radiation dose level on the detectability of pulmonary nodules in chest tomosynthesis. Eur Radiol 2014; 24: 1529-36.
64. Teramoto A, Tsujimoto M, Inoue T, Tsukamoto T, Imaizumi K, Toyama H, et al. Automated Classification of Pulmonary Nodules through a Retrospective Analysis of Conventional CT and Two-phase PET Images in Patients Undergoing Biopsy. Asia Ocean J Nucl Med Biol 2019; 7: 29-37.
65. MacMahon H, Naidich DP, Goo JM, Lee KS, Leung ANC, Mayo JR, et al. Guidelines for management of incidental pulmonary nodules detected on CT images: from the fleischner society 2017. Radiology 2017; 284: 228-43.

8 APPENDICES

8.1 APPENDIX 1

Gradation Processing (GP)	
Gradation Amount (GA)	Adjustment of the contrast. As the numeric value increases, the contrast becomes enhanced
Gradation Type (GT)	A non-linear gradation curve, e.g. “e” curve represents for chest protocol
Gradation Center (GC)	Center for a density when GA value is changed
Gradation Shift (GS)	Adjustment of the density, at the numeric value increases, the density becomes enhanced;
Multi-objective Frequency Processing (MFP)	
Multi-Frequency Balance (MRB)	A factor that determines frequency band when applying image enhancement
Multi-DRC Balance Type (MDB)	A factor that determines the dynamic range (DR) compression processing
Multi-DRC Enhancing Type (MDT)	A factor that determines density area of DR compression processing
Multi-DRC Enhancement (MDE)	Degree of multi-DRC enhancement
Multi-Frequency Enhancing Type (MRT)	A non-linear curve which changes the degree of enhancement according to the image density
Multi-Frequency Enhancement (MRE)	The factor of adjustment of multi-frequency enhancement.
Flexible Noise Control (FNC)	
Filter Control of FNC (FFC)	To determine to what extent FNC is to be applied depending on the X-ray radiation dose
Balance Type of FNC (FNB)	To determine to what extent FNC is to be applied in relation to frequency components
The Type of FNC (FNT)	To determine to what extent FNC is to be applied to image density
The Enhancement of FNC (FNE)	To determine to what extent FNC is to be applied

8.2 APPENDIX 2

Tomosynthesis exposure ID	SID (cm)	Tube swing angle (°)	Total exposure time (s)	No. of exposures	Tube voltage kV	Tube current per projection [mA]	Projection time [s]
60	130	10	6.3	32	120	100	0,008
61	130	13	4.0	20	120	159	0,008
62	130	15	4.7	24	120	133	0,008
65	130	20	6.3	32	120	100	0,008
66	130	25	7.9	39	120	83	0,008
70	180	10	8.8	44	120	135	0,008
71	180	14	6.0	30	120	200	0,008
73	180	15	6.6	33	120	181	0,008
74	180	20	8.8	44	120	138	0,008
76	180	27	12.0	60	120	104	0,008

8.3 APPENDIX 3

Region	Structure	Criterion
A	Basal dorsal	Vessel demarcation (small vessels)
	Basal dorsal	Disturbance of vessels in front/behind
B	Spine	Definition of structure
C	Nodule	Homogeneous
	Nodule	Definition of edge
D	Peripheral vessels (upper, lateral right)	Vessel demarcation (small vessels)
	Peripheral vessels (upper, lateral right)	Disturbance of vessels in front/behind
E	Retrocardiac	Vessel demarcation
	Retrocardiac	Disturbance of vessels in front/behind
F	Carina	Definition of structure
G	Vessel round nodule	Vessel demarcation (3 mm vessels)
	Vessel round nodule	Disturbance of vessels in front / behind
H	Basal ventral	Vessel demarcation (small vessels)
	Basal ventral	Disturbance of vessels in front / behind

8.4 APPENDIX 4

Criteria	Structure
Demarcation	**Basal dorsal**, vessel demarcation (small vessels)
	Basal ventral, vessel demarcation (small vessels)
	Peripheral vessels, (upper, lateral right), vessel demarcation (small vessels)
	Retrocardiac, Vessel demarcation, Vessel demarcation (small vessels)
Disturbance	**Basal dorsal**, Disturbance of vessels in front / behind
	Peripheral vessels (upper, lateral right), Disturbance of vessels in front/behind
	Retrocardiac, Disturbance of vessels in front / behind
	Basal ventral, Disturbance of vessels in front / behind
Structure	Definition of bone structures in the spine